ELSEVIER

www.elsevier.nl/locate/jorganchem

Journal of Organometallic Chemistry 611 (2000) 551–557

Journal of Organo metallic Chemistry

Synthesis and characterization of N-confused porphyrinatoantimony(V): toward a low energy gap molecular wire

Takuji Ogawa [a,*], Hiroyuki Furuta [b], Minako Takahashi [a], Ayako Morino [a], Hidemitsu Uno [c]

[a] *Department of Chemistry, Faculty of Science, Ehime University, Matsuyama 790-8577, Japan*
[b] *Department of Chemistry, Graduate School of Science, Kyoto University, Kyoto 606-8502, Japan*
[c] *Advanced Instrumentation Center for Chemical Analysis, Ehime University, Matsuyama 790-8577, Japan*

Received 18 April 2000; accepted 22 April 2000

Abstract

N-Confused tetraarylporphyrinatoantimony(V) dimethoxides were synthesized and their X-ray crystallographic structure, absorption spectra and voltammetric spectra were studied. X-ray crystallographic structure revealed neutral molecules with no counter anion. From the absorption spectra and voltammetric studies we estimated their energy gaps to be about 0.2 eV less than the corresponding porphyrinatoantimony(V). The axial ligands could easily be exchanged in solvent alcohol by acid promotion. These characteristics of N-confused porphyrinatoantimony(V) indicate that they are good candidates for the molecular wire component. © 2000 Elsevier Science S.A. All rights reserved.

Keywords: N-Confused porphyrin; Antimony; Molecular wire

---

1. Introduction

The term 'molecular wire' is used for molecules that are electronically conductive with a highly preferred axis for conduction. The mechanism of conduction through a single molecule is quite different from that of the bulk organic conductive materials. In the latter the charges are carried by soliton in most cases. In contrast, conduction through single molecules generally involves tunneling or a resonant tunneling mechanism [1]. The resistance through a molecule of length L with an energy gap Eg is roughly estimated as $R \sim (12.9\ \mathrm{k\Omega})\exp(0.7245)\sqrt{Eg(\mathrm{eV})}L(\mathrm{\mathring{A}})$ [2]. According to this equation, the tunneling resistance will be less when the Eg of the molecule is smaller. Porphyrin wires are potentially highly conductive since they have a low Eg, as is easily predicted from their deep color. We have synthesized *meso–meso* coupled porphyrin arrays as good candidates for a molecular wire [3]. Although the solubility of the arrays was high even for long wires, one disappointment is that the electronic resonance between the porphyrin π-systems was not efficient because the porphyrin planes in the arrays are almost perpendicular to each other, and the energy gap did not decrease when the arrays were elongated [4]. Another possible method to make long porphyrin wires while keeping both the good resonance and high solubility is to connect them in an axial direction [5]. The semi-empirical molecular orbital calculation for the system in Fig. 1 showed that the resonance between the porphyrin moieties is feasible, and the Eg of the system steadily decreases when the arrays become longer, and as the central element became heavier, the Eg of the molecule became smaller.

Although the arrays of the Group 15 element complexes of porphyrins are promising as a molecular wire in this sense, counter anions present in these molecules will disturb the precise analysis of the electronic properties. In the Group 15 element porphyrins, the central elements are formally cationic, since porphyrins act as dianionic ligands when complexing. Thus, the position

---

* Corresponding author. Fax: +81-89-9279590.
E-mail address: ogawat@dpc.ehime-u.ac.jp (T. Ogawa).

0022-328X/00/$ - see front matter © 2000 Elsevier Science S.A. All rights reserved.
PII: S0022-328X(00)00405-8

of the counter ion in the molecule, which will affect the electronic properties considerably, remains ambiguous.

An 'N-confused porphyrin' (NCP; e.g. **1** and **2**) is a porphyrin isomer wherein one of the four pyrrole rings is inverted [6]. Recently, both theoretical [7] and experimental [8] studies have been reported on such exotic porphyrins that possess three nitrogens and one carbon as chelating donor atoms. The NCPs can behave both as a dianionic ligand ($\mathbf{P}^{2-}$) and as a trianionic ligand ($\mathbf{P}^{3-}$) when complexing with metal ions. If NCP works as $\mathbf{P}^{2-}$ for a Group 15 element, the central element of the product will be cationic, and if it acts as $\mathbf{P}^{3-}$ the central element will be electronically neutral. We have synthesized antimony complexes of N-confused tetraarylporphyrins as an initiatory step, and studied their structure and properties to elucidate their potential as components of highly conductive molecular wires (Chart 1).

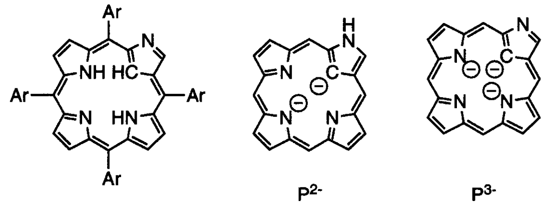

1: Ar =Ph
2: Ar =Tol

Chart 1.

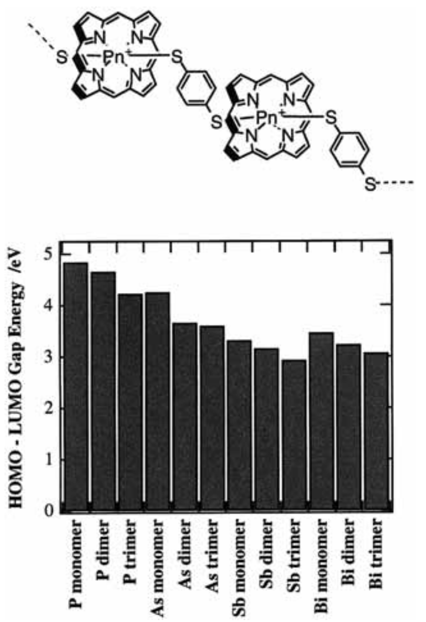

Fig. 1. PM3 calculated HOMO–LUMO energy gap of oligomeric porphyrinato pnictogenides(V). 'P monomer' indicates the molecule of HSC_6H_4S–porphyrinato phosphine(V)–SC_6H_4SH (will be abbreviated as HSC_6H_4S–Por–SC_6H_4SH) in which the sulfur atoms coordinate to the central phosphine. 'P dimer' indicates the molecule HSC_6H_4S–Por–SC_6H_4S–Por–SC_6H_4SH, and 'P trimer' means HSC_6H_4S–Por–SC_6H_4S–Por–SC_6H_4S–Por–SC_6H_4SH. 'As monomer' is the same as 'P monomer' except that the central atom is arsine. Other abbreviations were named in the same way.

2. Results and discussion

2.1. Reaction of N-confused porphyrins with $SbBr_3$

Semi-empirical molecular orbital calculations (PM3) performed in the system depicted in Chart 2 predicted that the cationic structure (**3**) would be about 13 kcal mol^{-1} more stable than the neutral one (**4** + HBr).

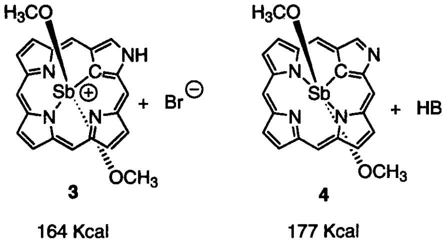

Chart 2.

However, in reality the reaction of N-confused tetraphenylporphyrin (**1**) with antimony(III) bromide in dry pyridine, followed by column chromatography using methanol–dichloromethane as the eluents afforded dimethoxy-coordinated N-confused tetraphenylporphyrinatoantimony(V) (**5**) (Scheme 1). The reaction of N-confused tetrakis(4-methylphenyl)porphyrin (**2**) with antimony(III) bromide in dry pyridine also afforded the corresponding product **6**. ^{1}H-NMR spectra of these products are consistent with the neutral structures **5** and **6**. If the N-confused porphyrin works as $\mathbf{P}^{2-}$, the outer C–H of the inverted pyrrole ring should be a doublet because of the spin coupling with the outer N–H. Actually, in N-confused porphyrinatopalladium(II) the outer C–H of the inverted pyrrole appeared as a doublet at δ 8.44 with a coupling constant of 2.9 Hz. However, in these cases the outer C–H were singlets (**5**, δ 9.83 and **6**, δ 9.84), indicating that there are no adjacent N–H protons in these molecules. The neutral structure was further confirmed by a single-crystal X-ray crystallographic analysis of **6** showing that no counter anion was present in the crystal (Fig. 2). Crystallographic data are shown in Table 1.

2.2. Comparison of $[Sb(NCTTP)(OCH_3)_2]$ (**6**) with $[Sb(TTP)(OCH_3)_2]$ (**7**)

It is interesting to compare the physical properties of **6** with **7** in which only the charge of the central element is different while the structure remains almost identical.

As abbreviated in Table 2, in the ^{1}H-NMR spectra the axial methoxy group appeared at δ −1.58 for **6** and −2.05 for **7**, and the β-proton of the pyrrole ring exhibited at δ 8.83–9.15 for **6** and 9.58 for **7**. These data show that the ring current generated by the aromatic π-electronic system is more effective in **7** than in **6**. In the non-symmetrical structure of **6**, the aromaticity seems to be decreased, probably because of the less

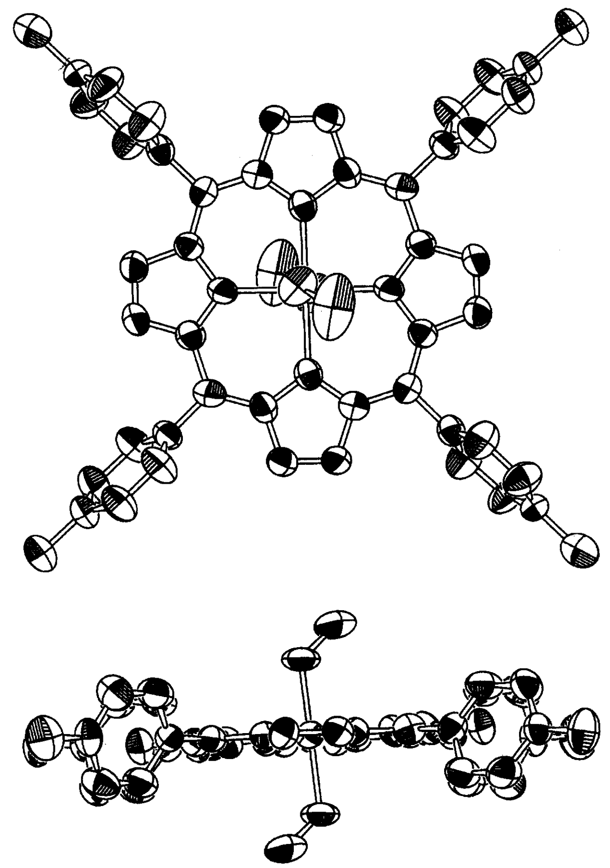

Fig. 2. X-ray crystallographic structure of **6**. Hydrogen atoms were removed for clarification. Because of small difference of electron density of nitrogen and carbon atoms, or disorder of the position of the inverted pyrrole ring, the position of the inverted nitrogen could not be determined by the X-ray crystallographic analysis. The bond length of O–Sb was 1.961(6) Å, which is ca. 0.02–0.03 Å longer than that of [Sb(TTP)(OCH(CH$_3$)$_2$)$_2$]Cl [12].

effective phase matching of the π-electronic system. Such weak aromaticity of the π-electronic system affects the chemical properties of N-confused porphyrins, and the 'inverted' pyrrole ring could be attacked easily by nucleophiles and/or electrophiles [8j,k].

In Fig. 3, cyclic and differential pulse voltammographs of compounds **6** and **7** are depicted, and the representative data are shown in Table 2. The first oxidation potential of [Sb(NCTTP)(OCH$_3$)$_2$] (**6**) (+690 mV vs. Ag/AgNO$_3$) was 850 mV lower than that of [Sb(TTP) (OCH$_3$)$_2$] (**7**) (+1540 mV vs. Ag/AgNO$_3$), and the first reduction potential of **6** (−1400 mV vs. Ag/AgNO$_3$) was 690 mV higher than that of **7** (−710 mV vs. Ag/AgNO$_3$). This is a reasonable consequence of the fact that the central element of **6** is neutral and that of **7** is cationic, and a cationic species is hard to oxidize and easy to reduce. An important result is that the $\Delta(E_{ox} - E_{red})$ is 160 mV smaller in **6** (2090 mV) than in **7** (2250 mV), that is, the energy gap of **6** is less than **7**.

The lower energy gap of **6** compared with **7** was also observed in the absorption spectrum shown in Fig. 4. The λ_{max} of the longest wavelength band of **6** is 683 nm (1.82 eV), while that of **7** is 610 nm (2.03 eV); the energy difference (0.21 eV) obtained from the absorption spectrum was consistent with the value obtained by voltammetric methods shown above (0.16 eV).

*2.3. Axial group exchange of [Sb(NCTTP)(OCH$_3$)$_2$] (**6**)*

When [Sb(NCTTP)(OCH$_3$)$_2$] (**6**) was refluxed in ethanol for 2 days, the axial group OCH$_3$ was exchanged

Table 1
Crystallographic Data for [Sb(NCTTP)(OCH$_3$)$_2$] (**6**)

Empirical formula	$C_{50}H_{42}N_4O_2Sb$
Formula weight	852.66
Space group	$P2_1/n$ (no. 14)
a (Å)	14.72(4)
b (Å)	9.795(4)
c (Å)	15.008(6)
α (°)	90
β (°)	90.87(4)
γ (°)	90
V (Å^3)	2163(6)
Z	2
D_{calc} (g cm^{-3})	1.315
μ(Mo–K$_\alpha$) (cm^{-1})	6.80
λ (Å)	0.71069
No. of reflections measured	Total: 5124, unique: 4163 [$R_{int} = 0.041$]
Structure solution	Direct methods
Refinement	Full-matrix least-squares on F^2
Function minimized	$\Sigma w(F_o^2 - F_c^2)^2$
Least squares weights	$w = 1/(\sigma^2(F_o^2)$
No. of observations ($I > 1.00\sigma(I)$)	3115
No. of variables	259
Reflection/parameter ratio	12.03
Residuals: R; R_w	0.115; 0.174
R_1	0.058
Goodness-of-fit indicator	1.28
Maximum peak in final difference map (e Å^{-3})	1.53
Minimum peak in final difference map (°)	−0.74

Table 2
Comparison of [Sb(NCTTP)(OCH$_3$)$_2$] (**6**) with [Sb(TTP) (OCH$_3$)$_2$] (**7**)

		6	**7**
^{1}H-NMR	Axial –OCH$_3$	−1.58	−2.05
	β proton of pyrrole	8.83∼9.15	9.58
Electrochemical vs. potential Ag/AgNO$_3$	$E_{ox}1$ (mV)	+690	+1540
	$E_{red}1$ (mV)	−1400	−710
	$\Delta(E_{ox}1 - E_{red}1)$ (mV)	2090	2250
Lowest absorption band	λ_{max} (nm)	683	610
	λ_{max} (eV)	1.82	2.03

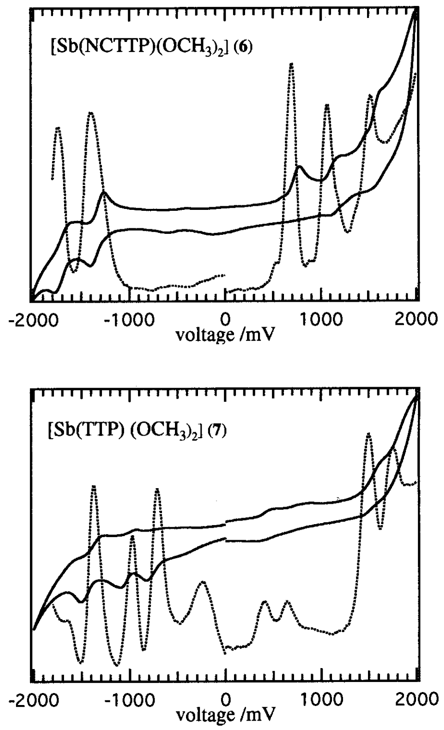

Fig. 3. Voltammographs of **6** and **7**. Solid lines show the cyclic voltammograph and broken lines indicate the differential pulse voltammograph. Working electrode, Pt disk; counter electrode, Pt wire; reference electrode, Ag/AgNO$_3$ in CH$_3$CN; solvent CH$_2$Cl$_2$; electrolyte, tetrabutylammonium perchlorate. Cyclic voltammograms were measured with a scan rate of 100 mV s^{-1}, and differential pulse voltammograms were obtained with the following conditions: Scan rate, 20 mV s^{-1}; pulse amplitude, 50 mV; sample width, 17 ms; pulse width, 50 ms; pulse period, 200 ms; quiet time, 2 s.

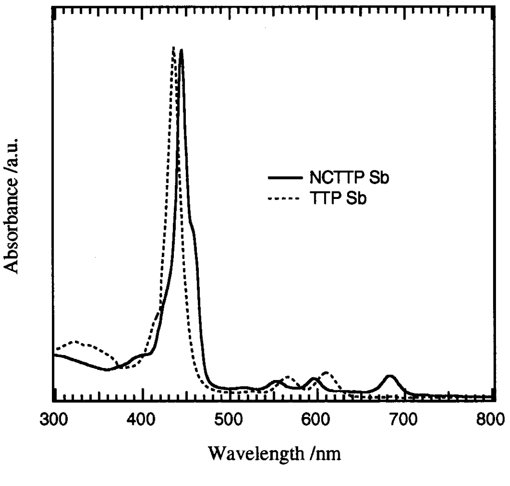

Fig. 4. Absorption spectra of **6** and **7** in CH$_2$Cl$_2$.

with OCH$_2$CH$_3$ to give [Sb(NCTTP)(OCH$_2$CH$_3$)$_2$] (**8**) quantitatively. Fig. 5 illustrates the time course of the exchange reaction probed by ^{1}H-NMR spectroscopy. Compound **6** was dissolved in 10% CDCl$_3$–CD$_3$OD and monitored by ^{1}H-NMR spectroscopy. As the axial CH$_3$O– group was exchanged with the CD$_3$O– of the solvent, the intensity of the CH$_3$O– group peak decreased slowly at room temperature (open circles in Fig. 5). In another run, CF$_3$COOH was added to the solution about 20 min after the sample was dissolved in the solvent. Before addition of the acid, the exchange reaction was slow, however, after the addition of the acid the reaction was accelerated, and 10 min after the addition more than 80% of the starting material **6** was converted into the deuterated compound. A total of 30 min after the addition the exchange of CH$_3$O– into CD$_3$O– was complete, and only a trace amount of the starting **6** could be observed (closed circle in Fig. 5) (Scheme 1).

Such a facile exchange of the axial groups was not observed for **7**. Scheme 2 shows a probable mechanism to explain the difference in the reactivity between porphyrinatoantimony and N-confused porphyrinatoantimony. The acid promotion of the exchange reaction indicates that this is an 'SN1-like' reaction and that the cationic species **A** must be involved as the key intermediate. In the case of **6**, the starting molecule is electronically neutral, and the cationic intermediate **A** can be stabilized by resonance with the N-confused porphyrin π-electronic system. In contrast, in the case of **7**, the starting molecule itself is cationic and the doubly positive charge at the antimony atom in an intermediate like **A** will destabilize the system greatly, and the exchange reaction must be retarded.

Such an easy ligand exchange will be useful in making long molecular wires; mixing **6** with the linking diol or dithiol molecules will make long molecules connected in axial directions, as illustrated in Fig. 1. A preliminary reaction of **6** with 1,2-ethylenediol was carried out to give the corresponding dimer and trimer. These results will be reported elsewhere.

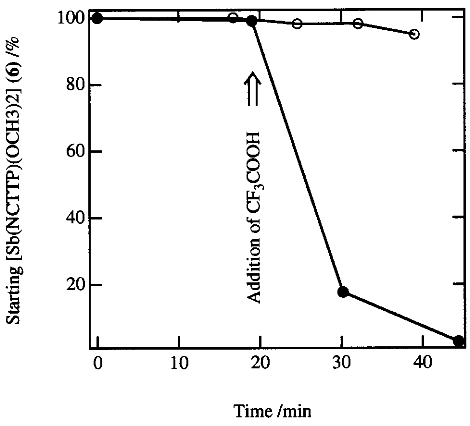

Fig. 5. Time course of the axial exchange reaction of **6** with CD$_3$O– group. Open circles represent the reaction without acid, and closed circles are the acid-promoted reaction. In the latter run, the acid was added ca. 20 min after the compound was dissolved in the solvent. The reactions were monitored by ^{1}H-NMR in ca. 10% CDCl$_3$–CD$_3$OD. The consumption of the starting material **6** was determined by the ratios of the integral areas of axial CH$_3$O– groups and methyl of the *meso*-tolyl groups. The probe temperature was 27°C.

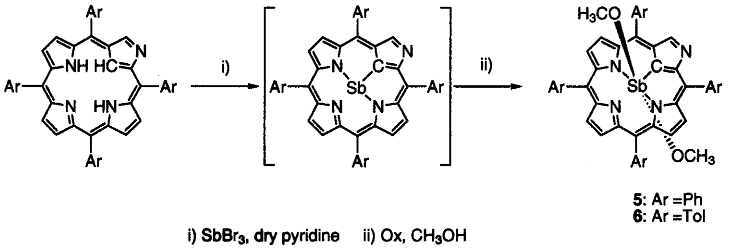

Scheme 1.

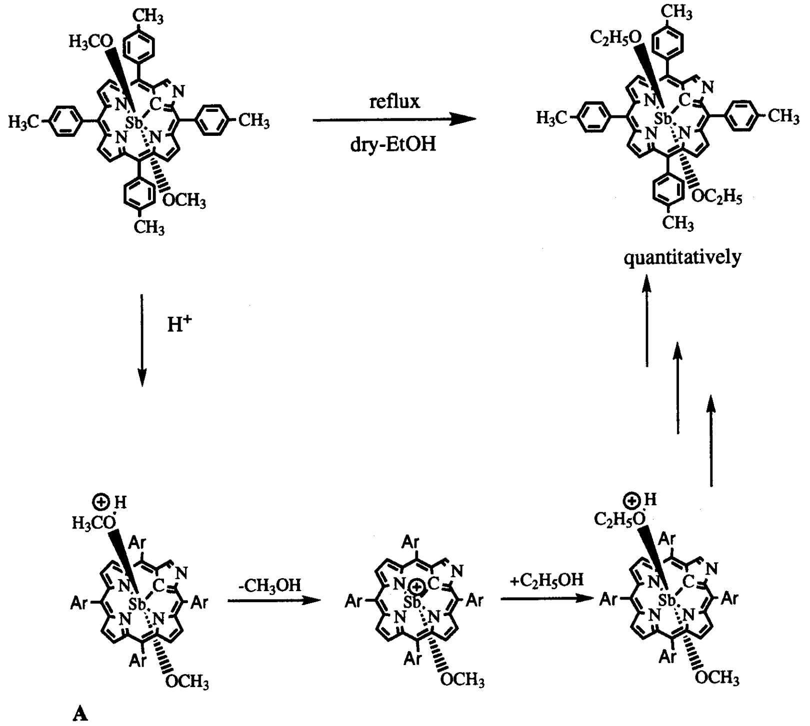

Scheme 2.

Here we have found that (1) N-confused porphyrinatoantimony(V) is a neutral molecule having no counter ion; (2) the energy gap of the molecule is about 0.2 eV less than the corresponding porphyrinatoantimony(V), and (3) the linkage of the molecule in the axial directions will be facile because of the easy axial ligand exchange. These characteristics of N-confused porphyrinatoantimony(V) indicate that they are good candidates for the molecular wire component.

3. Experimental

^{1}H-NMR (270 MHz) NMR spectra were recorded on a JEOL JNM-GSX270 and a JEOL JNM-EX. ^{1}H chemical shifts are referenced to internal tetramethylsilane (0 ppm). UV–vis spectra were recorded with JASCO V-570. Voltammetric measurements were performed with BAS CV-50WS. The working, auxiliary and reference electrodes were, respectively, a platinum disk, a platinum wire and an Ag/Ag$^+$ 0.010 M electrode. Mass spectra were measured on a JEOL JMS-LX2000. Melting points were measured with a Yanako BY-1. The elemental analyses were performed at the Microanalysis Division of the Advanced Instrumentation Center for Chemical Analysis, Ehime University.

Antimony(III) bromide, bromine, hydrogen bromide solution, methanol, dichloromethane were used as received. Pyridine was distilled under nitrogen from calcium hydride. N-Confused tetraarylporphyrins were prepared according to methods in the literature [6,9].

*3.1. Synthesis of N-confused tetraphenylporphyrinatoantimony(V) dimethoxide (**5**)*

A solution of N-confused tetraphenylporphyrin (61 mg, 0.1 mmol) and antimony(III) bromide (420 mg, 1.2 mmol) in dry pyridine (5 cm^3) was stirred under nitrogen for 24 h. The solvent was removed under vacuum, and the solute was purified by passing through an alumina chromatography column, followed by a silica-gel chromatography column using dichloromethane–methanol as the eluents. The product was recrystallized from dichloromethane–methanol to give purple crystals of **5** (27 mg, 34% isolated yield): m.p. > 270°C. ^{1}H-NMR: δ -1.59 (s, 6H, OCH_3), 7.77–8.23 (m, 20H, phenyl), 8.84–9.16 (m, 7H), 9.84 (s, 1H, C*H*=N of the inverted pyrrol). EIMS (70eV) *m*/*e* 795 [M^+, 4], 732 [100, $M^+ - (CH_3O)_2$]. UV–vis (CH_2Cl_2) λ_{max} 444, 552, 592, 680 nm.

*3.2. Synthesis of N-confused tetrakis(4-methylphenyl)porphyrinatoantimony(V) dimethoxide **(6)***

A solution of N-confused tetrakis(4-methylphenyl)-porphyrin (67 mg, 0.1 mmol) and antimony(III) bromide (420 mg, 1.2 mmol) in dry pyridine (5 cm^3) was stirred under nitrogen for 24 h. The solvent was removed under vacuum, and the solute was purified by passing through an alumina chromatography column, followed by a silica-gel chromatography column using dichloromethane–methanol as the eluents. The product was recrystallized from dichloromethane–methanol to give purple crystals of **6** (38 mg, 42% isolated yield): m.p. > 270°C. ^{1}H-NMR: δ -1.58 (s, 6H, OCH_3), 2.66 (s, 3H, CH_3), 2.69 (s, 3H, CH_3), 2.70 (s, 6H, $2CH_3$), 7.57–7.60 (m, 8H, aryl), 8.07–8.15 (m, 8H, aryl), 8.84–8.90 (m, 4H), 9.12–9.17 (m, 2H), 9.84 (s, 1H, C*H*=N of the inverted pyrrol). FABMS (*m*-nitrobenzyl alcohol) *m*/*e* 851 [M^+], 819 [$M^+ - CH_3OH$], 789 [$M^+ - 2(CH_3O){-}H$]. UV–vis (CH_2Cl_2) λ_{max} 445, 553, 596, 683 nm.

*3.3. X-ray crystal structure analysis of **6***

Single crystals were obtained by recrystallization from MeOH–CH_2Cl_2. Intensity data were collected on a Rigaku AFC7S diffractometer using a $\omega - 2\theta$ scan technique to a maximum 2θ value of 45.0°. Of the 5124 reflections that were collected, 4163 were unique. The structure was solved by direct methods [10] and expanded using Fourier analysis [11]. The non-hydrogen atoms were refined anisotropically. Hydrogen atoms were included but not refined. The final cycle of full-matrix least-squares refinement on F^2 was based on 3115 observed reflections ($I > 1.00\sigma(I)$) and 259 variable parameters and converged (the largest parameter shift was 12.03 times its estimated S.D.) with unweighted and weighted agreement factors of: $R = \Sigma(F_o^2 - F_c^2)/\Sigma F_o^2 = 0.115$, $R_w = [\Sigma w(F_o^2 - F_c^2)^2/\Sigma w(F_o^2)^2]^{1/2} = 0.174$, and $R_1 = \Sigma\|F_o| - |F_c\|/\Sigma|F_o| = 0.058$. The maximum and minimum peaks on the final difference Fourier map corresponded to 1.53 and -0.74 e Å^{-3}, respectively. All calculations were performed using the TEXSAN crystallographic software of the Molecular Structure Corporation. The crystal data and analytical conditions and final atomic coordinates and isotropic temperature factors are listed in Table 1.

*3.4. Axial ligand exchange of N-confused tetraphenylporphyrinatoantimony(V) dimethoxide **(5)***

N-Confused tetraphenylporphyrinatoantimony(V) dimethoxide (**5**) (82 mg, 0.1 mmol) was refluxed in ethanol (10 cm^3) for 2 days. After the solvent was removed in vacuo the product was purified by silica-gel column chromatography to give N-confused tetraphenylporphyrinatoantimony(V) diethoxide (**8**) in quantitative yield; ^{1}H-NMR ($CDCl_3$): δ -2.17 (t, $J = 7$ Hz, 6H), -1.57 (q, $J = 7$ Hz, 4H), 7.77–8.22 (m, 20H, phenyl), 8.81–9.12 (m, 6H), 9.83 (s, 1H, C*H*=N of the inverted pyrrol). FABMS (3-nitrobenzylalcohol) *m*/*z* 777 [$M^+ - CH_3CH_2OH$, 16%], 733 [$M^+ - 2(CH_3CH_2O){-}H$, 55%].

*3.5. Axial ligand exchange of N-confused tetrakis(4-methylphenyl)porphyrinato-antimony(V) dimethoxide **(6)***

N-Confused tetrakis(4-methylphenyl)porphyrinato-antimony(V) dimethoxide (**6**) (85 mg, 0.1 mmol) was refluxed in ethanol (10 cm^3) for 2 days. After the solvent was removed in vacuo the product was purified by silica-gel column chromatography to give N-confused tetrakis(4-methylphenyl)porphyrinato-antimony(V) diethoxide (**9**) in quantitative yield; ^{1}H-NMR ($CDCl_3$): δ -2.17 (t, $J = 7$ Hz, 6H), -1.57 (q, $J = 7$ Hz, 4H), 2.66 (s, 3H, CH_3), 2.69 (s, 3H, CH_3), 2.70 (s, 6H, $2CH_3$), 7.57–7.60 (m, 8H, aryl), 8.07–8.15 (m, 8H, aryl), 8.84–8.90 (m, 4H), 9.12–9.17 (m, 2H), 9.84 (s, 1H, C*H*=N of the inverted pyrrol).

4. Supplementary material

Complete lists of bond lengths and angles, hydrogen atom coordinates and anisotropic thermal parameters have been deposited at the Cambridge Crystallographic Data Centre (No. CCDC-143383). Copies of this information may be obtained free of charge from: The Director, CCDC, 12 Union Road, Cambridge, CB2 1EZ, UK (fax: +44-1223-336033; e-mail: deposit@ccdc.cam.ac.uk or www: http://www.ccdc.cam.ac.uk).

Acknowledgements

This work was supported by a Grant-in-Aid for Scientific Research (No. 11120240) from the Ministry of Education, Science, Sports, and Culture of the Japanese government.

References

[1] (a) V. Mujica, M. Kemp, A. Roitberg, M. Ratner, J. Chem. Phys. 104 (1996) 7296. (b) M. Di Ventra, S.T. Pantelides, N.D. Lang, Phys. Rev. Lett. 84 (2000) 979.

[2] M.P. Samanta, W. Tian, S. Datta, J.I. Henderson, C.P. Kubiak, Phys. Rev. B 53 (1996) R7626.

[3] T. Ogawa, Y. Nishimoto, N. Yoshida, N. Ono, A. Osuka, J. Chem. Soc. Chem. Commun. (1998) 337.

[4] T. Ogawa, Y. Nishimoto, N. Yoshida, N. Ono, A. Osuka, Angew. Chem. Int. Ed. Engl. 38 (1999) 176.

[5] (a) H. Segawa, N. Nakayama, T. Shimidzu, J. Chem. Soc. Chem. Commun. (1992) 784. (b) K. Kunimoto, H. Segawa, T. Shimidzu, Tetrahedron Lett. 33 (1992) 6327. (c) H. Segawa, K. Kunimoto, K. Susumu, M. Taniguchi, T. Shimidzu, J. Am. Chem. Soc. 116 (1994) 11193.

[6] (a) H. Furuta, T. Asano, T. Ogawa, J. Am. Chem. Soc. 116 (1994) 767. (b) P.J. Chmielewski, L. Latos-Grazynski, K. Rachlewicz, T. Glowink, Angew. Chem. Int. Ed. Engl. 33 (1994) 779.

[7] (a) J.L. Sessler, Angew. Chem. Int. Ed. Engl. 33 (1994) 1348. (b) A. Ghosh, Angew. Chem. Int. Ed. Engl. 34 (1995) 1028. (c) L. Szterenberg, L. Latos-Grazynski, Inorg. Chem. 36 (1997) 6287.

[8] (a) T. Ogawa, H. Nanami, N. Ono, H. Furuta, Pacifichem, Honolulu, 1995, # 1278, (b) P.J. Chmielewski, L. Latos-Grazynski, J. Chem. Soc. Perkin Trans. 2 (1995) 503. (c) K. Ariga, T. Kunitake, H. Furuta, J. Chem. Soc. Perkin Trans. 2 (1996) 667. (d) P.J. Chmielewski, L. Latos-Grazynski, T. Glowiak, J. Am. Chem. Soc. 118 (1996) 5690. (e) P.-Y. Hoo, K. Shin, C.-H. Lee, Tetrahedron Lett. 37 (1996) 197. (f) B.Y. Liu, C. Brückner, D. Dolphin, J. Chem. Soc. Chem. Commun. (1996) 2141. (g) Y. Ishikawa, I. Yoshida, K. Akaiwa, E. Koguchi, T. Sasaki, H. Furuta, Chem. Lett. (1997) 453. (h) P.J. Chmielewski, L. Latos-Grazynski, Inorg. Chem. 36 (1997) 840. (i) H. Furuta, T. Ogawa, Y. Uwatoko, K. Araki, Inorg. Chem. 38 (1999) 2676. (j) H. Furuta, T. Ishizuka, A. Osuka, T. Ogawa, J. Am. Chem. Soc. 121 (1999) 2945. (k) H. Furuta, H. Maeda, A. Osuka, J. Am. Chem. Soc. 122 (2000) 803.

[9] G.R. Geier, III, D.M. Haynes, J.S. Lindsey, Org. Lett. 1 (1999) 1455.

[10] SIR92: A. Altomare, M. Cascarano, C. Giacovazzo, A. Guagliardi, J. Appl. Crystallogr. 26 (1994) 343.

[11] DIRDIF-94: P.T. Beurskens, G. Admiraal, G. Beurskens, W.P. Bosman, R. de Gelder, R. Israel, J.M.M. Smits (1994). The DIRDIF-94 program system, Technical Report of the Crystallography Laboratory, University of Nijmegen, The Netherlands.

[12] T. Barbour, W.J. Belcher, P.J. Brothers, C.E. Rickard, D.C. Ware, Inorg. Chem. 31 (1992) 746.